Modeling and Nonlinear Robust Tracking Control of a Three-Rotor UAV Based on RISE Method

WEI HAO[1,2], WENLAI MA[1,2], WEI YUAN[1], HAIJUN WANG[1], AND YUJIE DU[1,2]
[1]Flying College, Binzhou University, Binzhou 256600, China
[2]Aviation Information Technology Research and Development Center, Binzhou University, Binzhou 256600, China

Corresponding author: Wei Hao (haowei0923@tju.edu.cn)

ABSTRACT In this paper, the flight principle and accurate dynamics of three-rotor unmanned aerial vehicle (UAV) are detailedly analyzed and a nonlinear robust tracking control strategy is proposed considering unknown time-varying external disturbances. Aiming at the tracking control of the typical underactuated system, the dynamic model of the three-rotor UAV is divided into outer-loop position subsystem and inner-loop attitude subsystem. The feedback linearization algorithm is employed to design the outer-loop controller for the trajectory tracking of the UAV. For the inner-loop control of the UAV, the robust integral of the signum of the error (RISE) method is utilized to formulate the robust attitude controller to deal with the external disturbances. The stability of the closed loop system and the asymptotical tracking of the desired trajectory are proved via Lyapunov based stability analysis. Real-time experiments are implemented to validate the performance of the proposed control strategy.

INDEX TERMS Three-rotor UAV, feedback linearization, RISE, robust tracking control.

I. INTRODUCTION

Over the past few years, the multi-rotor UAVs have shown great advantages in both military and civil applications [1]–[3], including surveillance, fire fighting and so on [4], [5]. Comparing with other common multi-rotor UAVs, such as quadrotor UAV and hexarotor UAV, the three-rotor UAV is a new configuration consisting of two fixed motors and one tilt motor that is equipped with a rear servo, which makes it possess some unique properties such as simpler structure, lower cost, lower energy consumption and higher maneuverability [6], shown as FIGURE 1.

As a new configuration of the multi-rotor UAV, the three-rotor UAV has attracted increasing attentions from different research institutes. In [7], the 6 degree-of-freedom (DOF) dynamic model for a three-rotor UAV is first obtained via the Newton-Euler approach, and then the saturating function based sequential control strategy is employed to achieve stabilization of its attitude and position, which is verified through real-time experiments on the self-build simulink-based platform. In [8], an accurate dynamic model is derived for a three-rotor UAV and the classical PID control law is developed for its stabilization control, which are finally

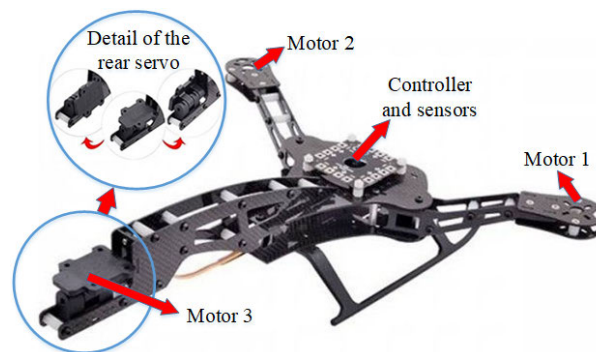The associate editor coordinating the review of this manuscript and approving it for publication was Shihong Ding [ID].

FIGURE 1. Structural framework of the three-rotor UAV.

verified via numerical simulations. In [9], the control scheme consisting of a PID based attitude control and a linear quadratic translational control for a three-rotor UAV is presented, and the numerical simulation results demonstrate the efficiency of both attitude and position control schemes. An adaptive hybrid control strategy based on fuzzy regulation, pole-placement and the tracking control algorithm demonstrated in [10] is utilized to design the attitude and altitude control law for a three-rotor UAV. The numerical simulation results show that the proposed controller has better

transient response with low overshoot and undershoot to achieve the desired attitude.

From the literatures mentioned above, it can be concluded that the current research interests of the three-rotor UAV are mainly focused on the dynamic modeling and flight control. Actually, the three-rotor UAV has 6 DOF with only four control inputs, which is known as the underactuated property [11]–[13], thus the tracking control [14], [15] design for a three-rotor UAV is a complex task. To deal with the underactuated property, the existing tracking control strategies for multi-rotor UAV can be mainly classified into backstepping based controllers [16] and inner-and-outer-loop based controllers [17]. The backstepping scheme has its standard structure and stability analysis, but the tuning of the control gains is not a easy task. The inner-and-outer-loop control strategy produces continuous input signals, while the stability analysis is more complicated. However, the existing FTC methodologies proposed for other UAVs, such as sliding mode control [18], adaptive control [19], [20], model predictive control [21] and so on, are very difficult to be applied on the three-rotor UAV directly.

In our previous work [22], a nonlinear robust fault tolerant position tracking control strategy is proposed for a three-rotor UAV to deal with the rear servo's stuck fault together with parametric uncertainties and unknown external disturbances. For the attitude control, an adaptive sliding mode observer is designed to estimate the unknown rear servo's stuck fault, and then the RISE [23] method is employed to compensate the estimation errors and exogenous disturbances. For the position control, the I&I methodology is utilized to compensate the parametric uncertainties. Finally, the real-time flight experiments validate the effectiveness of the proposed strategy.

Therefore, to address the aforementioned problems, the inner-and-outer-loop based control strategy is also applied in this paper for a three-rotor UAV, which is affected by unknown external time-varying disturbances. The feedback linearization method is employed to design the controller for the outer-loop (position loop) of the UAV, and the RISE method is utilized to formulate the robust controller for the inner-loop (attitude loop). Then a composite Lyapunov theory is employed to prove the stability of the closed-loop system and the asymptotic tracking of the desired position trajectory for the UAV. Finally, the proposed FTC strategy is verified through real-time flight experiments performed on the self-build HILS three-rotor UAV testbed.

The main contributions of this paper can be summarized as follows. Firstly, the detailed dynamics of the three-rotor UAV are taken into consideration, where the anti-torque produced by the rotors together exogenous disturbances are included, while most other existing works do not. Secondly, for the position loop control, the feedback linearization method is applied, and for the attitude loop, RISE based controller is developed to compensate the unknown exogenous time-varying disturbances to improve the robustness of the closed loop system and achieve a continuous control input. Finally, the proposed FTC strategy is verified through real-time flight experiments. To our best knowledge, few previous works from other research institutes have developed complete tracking control and stability analysis for the three-rotor UAV.

The rest of paper is organized as follows. The flight principle and dynamics of the three-rotor UAV with unknown time-varying disturbances are described in Section II. In Section III, the design of the tracing control scheme and composite stability analysis are presented. The real-time experimental results are shown in Section IV. Finally, some conclusion remarks are included in Section V.

II. DYNAMIC ANALYSIS OF THE THREE-ROTOR UAV
A. FLIGHT PRINCIPLE OF THE THREE-ROTOR UAV
As a new configuration of multi-rotor UAV, the three-rotor UAV's flight principle is quite distinctive, as illustrated in FIGURE 2. The roll motion is realized only by changing the speeds of motor 1 and motor 2. The pitch motion is realized by changing the speeds of all the three motors together with the deflection of the rear servo. Meanwhile, the yaw motion is also changed by the anti-torque produced by the three motors and the deflection of the rear servo.
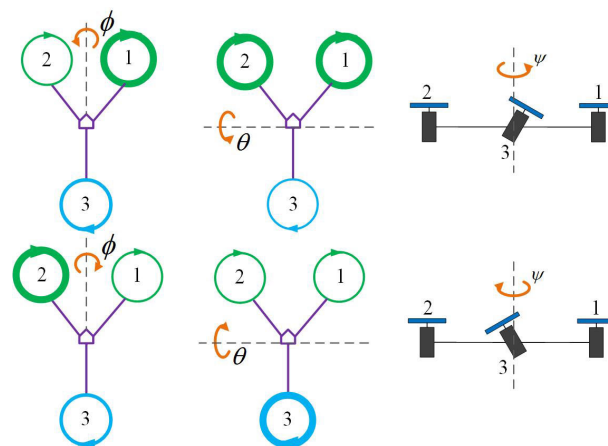

FIGURE 2. Flight principle of three-rotor UAV.

B. MATHEMATICAL MODEL OF THE THREE-ROTOR UAV
In order to describe the dynamics and kinematics of the three-rotor UAV, two right-hand coordinate systems are utilized. The inertial reference frame is denoted by $\{\mathcal{I}\}$, and the body-fixed reference frame is denoted by $\{\mathcal{B}\}$, as illustrated in FIGURE 3.

The origin of the orthogonal right-hand coordinate system $\{\mathcal{I}\}$ is attached on the ground, which can be represented by $\mathcal{I} = \{x_{\mathcal{I}}, y_{\mathcal{I}}, z_{\mathcal{I}}\}$ with $z_{\mathcal{I}}$ being the vertical direction upward into the sky, $y_{\mathcal{I}}$ being the west direction and $x_{\mathcal{I}}$ being determined by the right-hand rule. The frame $\mathcal{B} = \{x_{\mathcal{B}}, y_{\mathcal{B}}, z_{\mathcal{B}}\}$ represents an orthogonal right-hand coordinate system which is centered at the centroid of the three-rotor. The body axis $z_{\mathcal{B}}$ is the normal axis of the principal plane of three-rotor
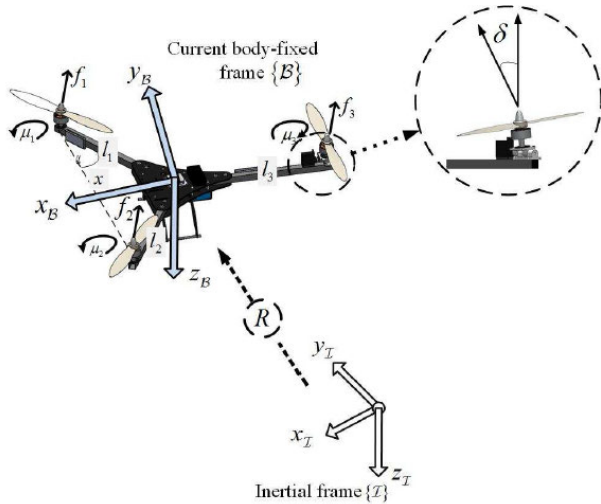
FIGURE 3. Schematic of the three-rotor UAV.

directed from bottom to top, the body axis x_B is along with the forward flying direction of the three-rotor, and the direction of the body axis y_B is determined by the right-hand rule. The dynamic model of the three-rotor UAV of mass $m \in \mathbb{R}^+$ and inertial $J \in \mathbb{R}^{3\times 3}$ can be illustrated via the following differential equation, expressed in the body-fixed reference frame $\{\mathcal{B}\}$:

$$\begin{cases} J\dot{\Omega} = -S(\Omega)J\Omega + \tau + \tau_d \\ m\ddot{\xi} = -FRe_3 + mge_3, \end{cases} \quad (1)$$

where $\Omega(t) = \begin{bmatrix} \omega_1(t) & \omega_2(t) & \omega_3(t) \end{bmatrix}^T \in \mathbb{R}^3$ denotes the angular velocity of the UAV in the body-fixed reference frame and $\xi(t) = \begin{bmatrix} x(t) & y(t) & z(t) \end{bmatrix}^T \in \mathbb{R}^3$ denotes the position with respect to the inertial reference frame. In (1), the vector $\tau(t) = \begin{bmatrix} \tau_\phi(t) & \tau_\theta(t) & \tau_\psi(t) \end{bmatrix}^T \in \mathbb{R}^3$ denotes the total rotational torque, the constant $F \in \mathbb{R}^+$ is the total thrust, the vector $\tau_d(t) \in \mathbb{R}^3$ is unknown external disturbances, the matrix $R \in \mathbb{R}^{3\times 3}$ is the rotation matrix from $\{\mathcal{B}\}$ to $\{\mathcal{I}\}$, the vector $e_3 = \begin{bmatrix} 0 & 0 & 1 \end{bmatrix}^T \in \mathbb{R}^3$ and the matrix $S(\cdot)$ represents the skew matrix which satisfies the following equation:

$$S(a) = \begin{bmatrix} 0 & -a_3 & a_2 \\ a_3 & 0 & -a_1 \\ -a_2 & a_1 & 0 \end{bmatrix}, \forall a = \begin{bmatrix} a_1 & a_2 & a_3 \end{bmatrix}^T. \quad (2)$$

In FIGURE 3, motor 1 and motor 2 rotate clockwise and motor 3 anticlockwise, and the symbols $f_i(t)$ and $\mu_i(t)$, $(i = 1, 2, 3)$ represent the thrust and anti-torque produced by the ith motor respectively. The constant $l_i, (i = 1, 2, 3)$ denotes the distance between the ith motor and the origin $O_\mathcal{B}$. Supposing there were a line connecting motor 1 to motor 2 and another connecting motor 1 the origin $O_\mathcal{B}$, then an angle would be formulated between these two lines which is denoted by α. The signal $\delta(t)$ represents the angle that the rear servo deviates from the plane of $X_\mathcal{B}O_\mathcal{B}Z_\mathcal{B}$, with clockwise being the positive direction.

Utilizing the thrust $f_i(t)$ and the anti-torque $\mu_i(t)$ to represent the total thrust $F(t)$ and $\tau(t)$, then the following equation can be obtained.

$$\begin{cases} [c]lF = -f_1 - f_2 - f_3 \cos \delta \\ \tau_\phi = f_1 l_1 \cos \alpha - f_2 l_2 \cos \alpha \\ \tau_\theta = -(f_1 l_1 + f_2 l_2) \sin \alpha + f_3 \cos \delta \cdot l_3 - \mu_3 \sin \delta \\ \tau_\psi = -\mu_1 - \mu_2 + \mu_3 \cos \delta + f_3 \sin \delta \cdot l_3. \end{cases} \quad (3)$$

Remark 1: If the motor speed is defined as $n_i(t)$, $i = 1, 2, 3$, then the vectors $f_i(t)$ and $\mu_i(t)$ can be obtained as

$$f_i = k_{fi} n_i^2, \quad i = 1, 2, 3, \quad (4)$$
$$\mu_i = k_{\mu i} n_i^2, \quad i = 1, 2, 3, \quad (5)$$

where k_{fi} and $k_{\mu i}$ are called lift coefficient and anti-torque coefficient respectively. Then the following equation can be concluded as

$$\mu_i = k_i f_i, \quad i = 1, 2, 3, \quad (6)$$

where $k_i = \frac{k_{\mu i}}{k_{fi}}$.

Assumption 1: The structure of the three-rotor UAV is symmetrical with respect to the axis of $O_\mathcal{B}X_\mathcal{B}$, so the equation of $l_1 = l_2 = l$ is established, where l is a constant.

Assumption 2: The three motors and propellers are of identical characteristics, therefore $k_1 = k_2 = k_3 = k$, where k is a constant.

Assumption 3: The terms of $\sin \delta$ can be neglected, since the angle $\delta(t)$ varies within a quite small range and $\sin \delta \ll \cos \delta$. Actually, the normal variation range of the angle $\delta(t)$ is bounded within $0.056 rad$.

When assumption 1, assumption 2 and assumption 3 are all satisfied, (3) and be rewritten as follows,

$$\begin{cases} F = -f_1 - f_2 - f_3 \cos \delta \\ \tau_\phi = (f_1 - f_2) l \cos \alpha \\ \tau_\theta = -(f_1 + f_2) l \sin \alpha + f_3 \cos \delta \cdot l_3 \\ \tau_\psi = -k(f_1 + f_2) + k_3 f_3 \cos \delta. \end{cases} \quad (7)$$

Assumption 4: For control design purposes, the attitude of three-rotor UAV is transformed into the inertial reference frame $\{\mathcal{I}\}$, which is represented by $\eta(t) = \begin{bmatrix} \phi(t) & \theta(t) & \psi(t) \end{bmatrix}^T \in \mathbb{R}^3$. The relationship between $\eta(t)$ and $\Omega(t)$ can be written as

$$\dot{\eta} = \Phi(\eta)\Omega, \quad (8)$$

where $\Phi(\eta)$ is called the Euler matrix and it is given by

$$\Phi(\eta) = \begin{bmatrix} 1 & \sin \phi \tan \theta & \cos \phi \tan \theta \\ 0 & \cos \phi & -\sin \phi \\ 0 & \sin \phi \sec \theta & \cos \phi \sec \theta \end{bmatrix}. \quad (9)$$

To avoid the singularity of the Euler matrix $\Phi(\eta)$, $\theta(t) \neq \pm \frac{\pi}{2}$ and its inverse matrix $\Psi(\eta) = \Phi^{-1}(\eta)$ is given by

$$\Psi(\eta) = \begin{bmatrix} 1 & 0 & -\sin \theta \\ 0 & \cos \phi & \cos \theta \sin \phi \\ 0 & -\sin \phi & \cos \theta \cos \phi \end{bmatrix}. \quad (10)$$

By differentiating (8) with respect to time and substituting the resulting equation into the first equation (1), we obtain

$$M(\eta)\ddot{\eta} + C(\eta, \dot{\eta})\dot{\eta} = \Psi^T(\eta)\tau + \Psi^T(\eta)\tau_d, \quad (11)$$

where the matrices $M(\eta)$ and $C(\eta, \dot{\eta})$ satisfy

$$M(\eta) = \Psi^T(\eta)J\Psi(\eta), \quad (12)$$
$$C(\eta, \dot{\eta}) = \Psi(\eta)J\dot{\Psi}(\eta) + \Psi(\eta)S(\Psi(\eta)\dot{\eta})J\Psi(\eta). \quad (13)$$

Recalling the second equation (1) and (11), the dynamics of the three-rotor UAV can be expressed as follows.

$$\begin{cases} m\ddot{\xi} = -FRe_3 + mge_3 \\ M(\eta)\ddot{\eta} + C(\eta, \dot{\eta})\dot{\eta} = \Psi^T(\eta)\tau + \Psi^T(\eta)\tau_d, \end{cases} \quad (14)$$

III. CONTROL DESIGN

Remark 2: Since the attitude dynamics in (14) is fully actuated for $\theta(t) \neq \pm\pi/2$, then it is exact feedback linearizable. By applying the change of variables

$$\begin{cases} \tau = J\Psi(\eta)u + \Phi^T C(\eta, \dot{\eta})\dot{\eta} \\ \tau_d = J\Psi(\eta)T_d, \end{cases} \quad (15)$$

the dynamics of the three-rotor UAV in (14) can be transformed into

$$\begin{cases} m\ddot{\xi} = -FRe_3 + mge_3 \\ \ddot{\eta} = u + T_d, \end{cases} \quad (16)$$

where $u(t) = \begin{bmatrix} u_\phi(t) & u_\theta(t) & u_\psi(t) \end{bmatrix}^T$, $T_d(t) = \begin{bmatrix} T_{d\phi}(t) & T_{d\theta}(t) & T_{d\psi}(t) \end{bmatrix}^T$.

Assumption 5: The unknown time-varying disturbance $T_d(t)$ is continuous differentiable and bounded up to its second order time derivative, i.e., $T_{di}(t) \in \mathfrak{L}^2$ for $i = \phi, \theta, \psi$.

Remark 3: From (16), the system can be divided into translation and rotation dynamics which are coupled through the rotation matrix R. In fact, the rotation dynamics do not depend on translation components but the translation dynamics depend on angles via the rotation matrix R. Since the overall control objective is to design a controller to ensure the accurate trajectory tracking for both attitude and position, the reference trajectories defined as $\begin{bmatrix} \xi_d(t) & \psi_d(t) \end{bmatrix}^T \in \mathbb{R}^4$ can fully achieve that. The reference roll and pitch angles defined as $\begin{bmatrix} \phi_d(t) & \theta_d(t) \end{bmatrix}^T \in \mathbb{R}^2$ will be computed through the position controller.

Remark 4: It should be mentioned that the control law is designed for the dynamic model (16), then the control for dynamic model (1) can be obtained through the first equation (15).

Let the desired position and attitude defined as $\xi_d(t) = \begin{bmatrix} x_d(t) & y_d(t) & z_d(t) \end{bmatrix}^T \in \mathbb{R}^3$ and $\eta_d(t) = \begin{bmatrix} \phi_d(t) & \theta_d(t) & \psi_d(t) \end{bmatrix}^T \in \mathbb{R}^3$ respectively. Let the tracking error be defined as $e_\xi(t) = \begin{bmatrix} e_x(t) & e_y(t) & e_z(t) \end{bmatrix}^T \in \mathbb{R}^3$ and $e_\eta(t) = \begin{bmatrix} e_\phi(t) & e_\theta(t) & e_\psi(t) \end{bmatrix}^T \in \mathbb{R}^3$ which can be calculated as

$$e_\xi = \xi - \xi_d, \quad (17)$$

$$e_\eta = \eta - \eta_d. \quad (18)$$

Define the new error signal $E_\xi(t) \in \mathbb{R}^6$ and $E_\eta(t) \in \mathbb{R}^6$ as

$$E_\xi = \begin{bmatrix} e_\xi & \dot{e}_\xi \end{bmatrix}^T, \quad (19)$$
$$E_\eta = \begin{bmatrix} e_\eta & \dot{e}_\eta \end{bmatrix}^T, \quad (20)$$

and the following expression can be obtained as

$$\begin{cases} \dot{E}_\xi = A_1 E_\xi + B_1(v - \ddot{\xi}_d) + B_1\Delta(\eta_d, e_\eta) \\ \dot{E}_\eta = A_2 E_\eta + B_2(u + T_d - \ddot{\eta}_d), \end{cases} \quad (21)$$

where $A_1 = A_2 = \begin{bmatrix} 0 & 0 & 0 & 1 & 0 & 0 \\ 0 & 0 & 0 & 0 & 1 & 0 \\ 0 & 0 & 0 & 0 & 0 & 1 \\ 0 & 0 & 0 & 0 & 0 & 0 \\ 0 & 0 & 0 & 0 & 0 & 0 \\ 0 & 0 & 0 & 0 & 0 & 0 \end{bmatrix}$, $B_1 = B_2 = \begin{bmatrix} 0 & 0 & 0 \\ 0 & 0 & 0 \\ 0 & 0 & 0 \\ 1 & 0 & 0 \\ 0 & 1 & 0 \\ 0 & 0 & 1 \end{bmatrix}$.

The vector $v(t) = \begin{bmatrix} v_x(t) & v_y(t) & v_z(t) \end{bmatrix}^T \in \mathbb{R}^3$ is a virtual control input which is defined as

$$v = -\frac{1}{m}F \cdot R(\eta_d)e_3 + ge_3, \quad (22)$$

and the vector $\Delta(\eta_d, e_\eta)$ represents the coupled terms between the UAV's attitude and position system.

In (22), the components of $v(t)$ are given by

$$\begin{cases} v_x = -\frac{1}{m}F(\cos\phi_d \sin\theta_d \cos\psi_d + \sin\phi_d \sin\psi_d) \\ v_y = -\frac{1}{m}F(\cos\phi_d \sin\theta_d \sin\psi_d - \sin\phi_d \cos\psi_d) \\ v_z = -\frac{1}{m}F \cos\theta_d \cos\phi_d + g. \end{cases} \quad (23)$$

Then from (23), the desired thrust and attitude are solved as

$$\begin{cases} F = m\sqrt{v_x^2 + v_y^2 + (g + v_z)^2} \\ \phi_d = \arcsin(\frac{m}{F}(v_1 \sin\psi_d - v_2 \cos\psi_d)) \\ \theta_d = \arctan(\frac{1}{v_3 + g}(v_1 \cos\psi_d + v_2 \sin\psi_d)). \end{cases} \quad (24)$$

After taking (18) into (16), (16) can be rewritten as

$$\ddot{\xi} = v + \delta(\eta_d, e_\eta), \quad (25)$$

where the vector $\delta(\eta_d, e_\eta)$ is defined as

$$\delta(\eta_d, e_\eta) = -\frac{1}{m}F \cdot Re_3 + ge_3 - v. \quad (26)$$

Now, the cascaded system (21) is obtained by computing the time derivative of both position and attitude tracking errors $(E_\xi(t), E_\eta(t))$ and recalling (25). To synthesize the control laws $v = f_1(E_\xi, \ddot{\xi}_d)$ and $u = f_2(E_\eta, \ddot{\eta}_d)$ for connected system (21), we will use the following theorem expressed by [26].

Theorem 1: If there is a feedback $v = f_1(E_\xi, \ddot{\xi}_d)$ such that $E_\xi = 0$ is an asymptotically stable equilibrium of the system $\dot{E}_\xi = A_1 E_\xi + B_1(v - \ddot{\xi}_d)$, then any partial state feedback control $u = f_2(E_\eta, \ddot{\eta}_d)$, which renders the E_η-subsystem

equilibrium $E_\eta = 0$ asymptotically stable, also achieves asymptotic stability of $(E_\xi, E_\eta) = (0, 0)$.

According to theorem 1, it states that partial-state feedback design can be applied to control system (21) by synthesizing two independent controllers $v = f_1(E_\xi, \ddot{\xi}_d)$ and $u = f_2(E_\eta, \ddot{\eta}_d)$, and the interconnection term $B_1\Delta(\eta_d, e_\eta)$ acts as a disturbance on the E_ξ-subsystem, which must be driven to zero. Thus, the outer-loop subsystem can be chosen as

$$\dot{E}_\xi = A_1E_\xi + B_1(v - \ddot{\xi}_d), \tag{27}$$

in which the coupling term $B_1\Delta(\eta_d, e_\eta)$ is temporarily not considered. The inner-loop subsystem can be chosen as

$$\dot{E}_\eta = A_2E_\eta + B_2(u + T_d - \ddot{\eta}_d). \tag{28}$$

Then the control objective is thus to design the control laws $v = f_1(E_\xi, \ddot{\xi}_d)$ and $u = f_2(E_\eta, \ddot{\eta}_d)$ such that the tracking errors $E_\xi(t)$ and $E_\eta(t)$ converge to zero asymptotically.

A. OUTER-LOOP CONTROL DESIGN

The objective of the outer-loop control is to design the control input $v(t)$ to ensure that the tracking error $E_\xi(t)$ converges to zero asymptotically. Consider system (27), we can use simple linear controllers which can be designed as

$$v = -K_\xi E_\xi + \ddot{\xi}_d, K_\xi \in \mathbb{R}^{3\times6}, \tag{29}$$

where the parameter K_ξ satisfies that $A_\xi = A_1 - B_1K_\xi$ is Hurwitz.

B. INNER-LOOP CONTROL DESIGN

The objective of the inner-loop control is to design a proper control scheme $u(t)$, which will ensure the asymptotic convergence of the tracking error $E_\eta(t)$ in (28). For convenience of the following control design, the filtered error signals $s_\eta(t) = \begin{bmatrix} s_\phi(t) & s_\theta(t) & s_\psi(t) \end{bmatrix}^T \in \mathbb{R}^3$, $r_\eta(t) = \begin{bmatrix} r_\phi(t) & r_\theta(t) & r_\psi(t) \end{bmatrix}^T \in \mathbb{R}^3$ are defined as follows:

$$s_\eta = \dot{e}_\eta + \alpha_\eta e_\eta, \tag{30}$$

$$r_\eta = \dot{s}_\eta + \beta_\eta s_\eta, \tag{31}$$

where $\alpha_\eta = diag\left\{\begin{bmatrix} \alpha_\phi & \alpha_\theta & \alpha_\psi \end{bmatrix}^T\right\} \in \mathbb{R}^{3\times3}$, $\beta_\eta = diag\left\{\begin{bmatrix} \beta_\phi & \beta_\theta & \beta_\psi \end{bmatrix}^T\right\} \in \mathbb{R}^{3\times3}$, and all the signals are some positive constant gains.

Take the roll channel as an example in the following analysis, it can be concluded that

$$s_\phi = \dot{e}_\phi + \alpha_\phi e_\phi, \tag{32}$$

$$r_\phi = \dot{s}_\phi + \beta_\phi s_\phi, \tag{33}$$

After taking the time derivative of $r_\phi(t)$ and substituting (18), (32) into the resulting equation, the following equation is obtained

$$\dot{r}_\phi = \dot{u}_\phi + \dot{T}_{d\phi} - \dddot{\phi}_d + \alpha_\phi \ddot{e}_\phi + \beta_\phi \dot{s}_\phi. \tag{34}$$

Let the auxiliary functions denoted by $N_\phi(\phi^{(i)}, t) \in \mathbb{R}$, $N_{d\phi}(t) \in \mathbb{R}$ and $\tilde{N}_\phi(t) \in \mathbb{R}$ be defined as follows:

$$N_\phi(\phi^{(i)}, t) = -\dddot{\phi}_d + \dot{T}_{d\phi} + \alpha_\phi \ddot{e}_\phi + \beta_\phi \dot{s}_\phi + s_\phi, \tag{35}$$

$$N_{d\phi}(t) = -\dddot{\phi}_d + \dot{T}_{d\phi}, \tag{36}$$

$$\tilde{N}_\phi(t) = N_\phi - N_{d\phi} = \alpha_\phi \ddot{\phi}_e + \beta_\phi \dot{s}_\phi + s_\phi. \tag{37}$$

Substituting (35)-(37) into (34), the open-loop error dynamics of the roll channel is obtained as

$$\dot{r}_\phi = -s_\phi + \dot{u}_\phi + N_{d\phi} + \tilde{N}_\phi. \tag{38}$$

Based on (38), the controller $u_\phi(t)$ is designed as

$$\dot{u}_\phi = -(g_\phi + 1)r_\phi - h_\phi sign(s_\phi). \tag{39}$$

where $g_\phi \in \mathbb{R}$ and $h_\phi \in \mathbb{R}$ are some positive gains.

Substituting (39) into (38), the closed-loop error dynamics of the roll channel is obtained as

$$\dot{r}_\phi = -s_\phi - (g_\phi + 1)r_\phi - h_\phi sign(s_\phi) + N_{d\phi} + \tilde{N}_\phi. \tag{40}$$

Remark 5: Since $\tilde{N}_\phi(s_\phi, r_\phi)$ is continuously differentiable, it satisfies the following inequality [27]

$$\left\| \tilde{N}_\phi(s_\phi, r_\phi) \right\| \le \rho_\phi(\eta_\phi) \left\| \eta_\phi \right\|, \tag{41}$$

where

$$\eta_\phi = \begin{bmatrix} s_\phi & r_\phi \end{bmatrix}^T \tag{42}$$

and the function $\rho_\phi(\cdot) : \mathbb{R}^+ \to \mathbb{R}^+$ is an invertible non-decreasing function.

C. STABILITY ANALYSIS

For the outer-loop control, it can be easily concluded that if $A_\xi = A_1 - B_1K_\xi$ is Hurwitz, then it can be obtained as

$$\lim_{t \to \infty} E_\xi(t) = 0. \tag{43}$$

i.e., $E_\xi(t)$ is asymptotically stable.

For the inner-loop control, the following theorem can be obtained.

Theorem 2: Considering the system (38), if the control gains h_ϕ is selected to satisfy the following condition

$$h_\phi > \left\| N_{d\phi} \right\|_\infty + \frac{1}{\beta_\phi} \left\| \dot{N}_{d\phi} \right\|_\infty, \tag{44}$$

then the control laws in (39) ensure the closed-loop system (40) to be semi-globally asymptotically stable.

Proof: Let the auxiliary function $A_{u\phi}(t) \in \mathbb{R}$ be defined as

$$A_{u\phi} = A_{0\phi} - \int_0^t r_\phi(\tau)(N_{d\phi}(\tau) - h_\phi sign(s_\phi(\tau)))d\tau, \tag{45}$$

where

$$A_{0\phi} = h_\phi \left| s_\phi(0) \right| - s_\phi(0)N_{d\phi}(0). \tag{46}$$

Based on the analysis in [27], it is not difficult to check that $A_{u\phi}(t) \ge 0$. Let the Lyapunov function candidate denoted by $V_\phi(\zeta_\phi, t) \in \mathbb{R}$ be defined as

$$V_\phi = \frac{1}{2}s_\phi^2 + \frac{1}{2}r_\phi^2 + A_{u\phi}, \tag{47}$$

where

$$\zeta_\phi = \left[\eta_\phi^T \;\; \sqrt{A_{u\phi}} \right]^T. \tag{48}$$

It is not difficult to check that $V_\phi(\zeta_\phi, t)$ is bounded by the following inequalities,

$$\frac{1}{2} \left\| \zeta_\phi \right\|^2 \leq V_\phi \leq \left\| \zeta_\phi \right\|^2. \tag{49}$$

After taking the time derivative of (47), and substituting (32), (40) together with (45) into the resulting equation, the following inequality can be obtained

$$\dot{V}_\phi \leq -k_{f\phi} \left\| \eta_\phi \right\|^2, \tag{50}$$

where

$$k_{m\phi} = \min\{\beta_\phi, 1\} \quad k_{f\phi} = k_{m\phi} - \frac{\rho_\phi^2(\eta_\phi)}{4g_\phi}. \tag{51}$$

If the control gain $k_{m\phi}$ satisfies the following inequality

$$k_{m\phi} > \frac{\rho_\phi^2(\eta_\phi)}{4g_\phi}, \tag{52}$$

it can be concluded that $k_{f\phi}(t) > 0$ and $\dot{V}_\phi(t) \leq 0$. Following the Lemma 2 in [27], let the auxiliary functions $W_{1\phi}(\zeta_\phi)$, $W_{2\phi}(\zeta_\phi)$ and $W_\phi(\zeta_\phi)$ be defined as

$$\begin{cases} W_{1\phi}(\zeta_\phi) = \frac{1}{2} \left\| \zeta_\phi \right\|^2 \\ W_{2\phi}(\zeta_\phi) = \left\| \zeta_\phi \right\|^2 \\ W_\phi(\zeta_\phi) = -k_{f\phi} \left\| \eta_\phi \right\|^2, \end{cases} \tag{53}$$

and the region D_ϕ be defined as

$$D_\phi = \{\zeta_\phi \in R^3 | \left\| \zeta_\phi \right\| < \rho_\phi^{-1}(2\sqrt{g_\phi k_{m\phi}})\}. \tag{54}$$

From (47) and (50), it can be concluded that $V(\zeta_\phi) \in \mathcal{L}_\infty$, thus $s_\phi(t) \in \mathcal{L}_\infty$ and $r_\phi(t) \in \mathcal{L}_\infty$. Then from (32), it is not difficult to know that $\dot{s}_\phi(t) \in \mathcal{L}_\infty$ and $\dot{e}_\phi(t) \in \mathcal{L}_\infty$. Furthermore, the boundedness of $\dot{u}_\phi(t) \in \mathcal{L}_\infty$ and $r_\phi(t) \in \mathcal{L}_\infty$ can be concluded from (34) and (39). From the definition of $W_\phi(\zeta_\phi)$, it can be concluded that $\dot{W}_\phi(\zeta_\phi) \in \mathcal{L}_\infty$, so $W(\zeta_\phi)$ is uniformly continuous. Let the convergence region denoted by S_ϕ be defined as

$$S_\phi : \{\zeta_\phi \in D_\phi, W_2(\zeta_\phi) < \frac{1}{2}(\rho_\phi^{-1}(2\sqrt{g_\phi k_{m\phi}}))^2\}. \tag{55}$$

Therefore, it can conclude that

$$\lim_{t \to \infty} \eta_\phi(t) = 0. \tag{56}$$

Then from (42), it can be obtained that

$$\lim_{t \to \infty} s_\phi(t) = 0, \; \lim_{t \to \infty} r_\phi(t) = 0. \tag{57}$$

Finally, from the linear filters in (32), it can be concluded that

$$\lim_{t \to \infty} e_\phi(t) = 0. \tag{58}$$

In the same way, it can also be concluded that

$$\lim_{t \to \infty} e_\theta(t) = 0, \; \lim_{t \to \infty} e_\psi(t) = 0. \tag{59}$$

From (43), (58) and (59), it can be concluded that all the conditions proposed in Theorem 1 are satisfied, then it can be concluded that

$$\lim_{t \to \infty} (E_\xi(t), E_\eta(t)) = (0, 0). \tag{60}$$

IV. EXPERIMENTAL RESULTS

To validate the performance of the proposed control scheme, real-time experiments are implemented on a HILS three-rotor UAV testbed as illustrated in [28]. The parameters of the three-rotor UAV are listed as $J = \left\{ \left[2.0 \; 8.3 \; 8.2 \right]^T \right\} \cdot 10^{-3} kg \cdot m^2$, $m = 0.5kg$, $l = 0.16m$, $l_3 = 0.25m$ and $\alpha = 26°$. The desired tracking position is selected as $x_d = 2\cos(\pi/100 \cdot t)$, $y_d = 2\sin(\pi/100 \cdot t)$, $z_d = 2m$, $\psi_d = 0$. The real-time experimental results of the FTC control scheme proposed in this paper are shown in FIGURE 4-FIGURE 6.
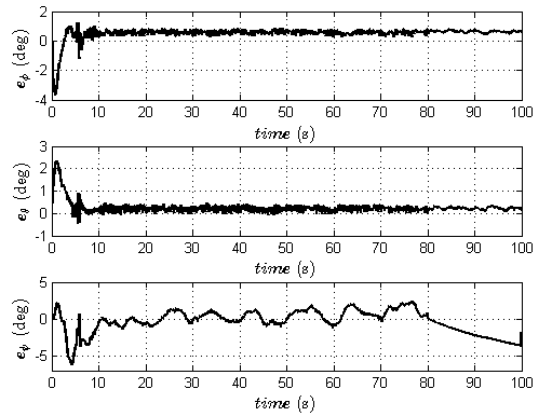
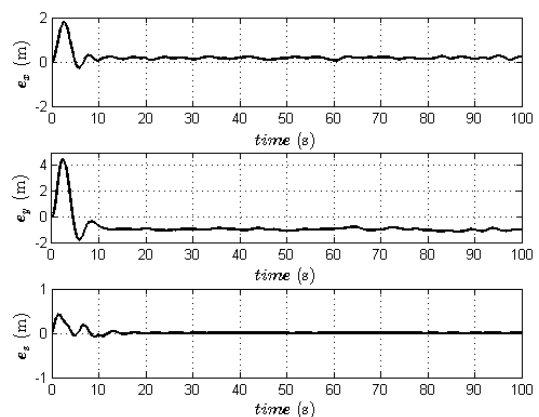**FIGURE 4.** UAV's attitude control errors.

FIGURE 5. UAV's trajectory tracking errors.

FIGURE 4 and FIGURE 5 show the UAV's attitude control errors and trajectory tracking errors respectively. In FIGURE 4, it's shown that the attitude tracking errors converge to 0 from the initial state within 5 seconds, and the control errors are bounded with $\pm 1°$. In FIGURE 5, the trajectory tracking errors are obtained by

substracting the desired position and the current position. Since the three-rotor UAV is fixed on a ball joint, the current position is obtained from the acceleration integral and the trajectory tracking control is validated through numerical simulations, while the attitude angles are measured via the UAV's onboard sensors.

The control inputs including the thrust produced by each motor and the rear servo's deflection angle are illustrated in FIGURE 6. The thrust is kept about $3N$ and the variation range of the rear servo's deflection angle is from $-20°\sim20°$ to maintain the torque balance.
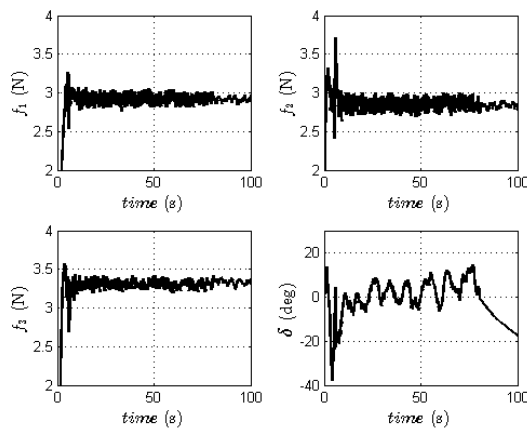

FIGURE 6. UAV's control inputs.

V. CONCLUSION

In this paper, a nonlinear robust tracking control scheme is developed to ensure the three-rotor UAV's trajectory tracking control under unknown time-varying disturbances. For the inner-loop (attitude loop) control, the RISE method is employed to compensate for the exogenous disturbances without the need of additional observer module. For the outer-loop (position) control, the feedback linearization methodology is utilized. The composite stability of the close-loop system is proved through Lyapunov-based methodology. Real-time experiments are performed on the self-build HILS testbed to show the effectiveness of the proposed control strategy. Future work will focus on the tracking control design of the three-rotor UAV considering output constraints and the full degree-of-freedom experimental verification.

REFERENCES

[1] B. Xian and W. Hao, "Nonlinear robust fault-tolerant control of the tilt trirotor UAV under rear servo's stuck fault: Theory and experiments," *IEEE Trans. Ind. Informat.*, vol. 15, no. 4, pp. 2158–2166, Apr. 2019.

[2] N. Gageik, P. Benz, and S. Montenegro, "Obstacle detection and collision avoidance for a UAV with complementary low-cost sensors," *IEEE Access*, vol. 3, pp. 599–609, Apr. 2015.

[3] F. Chen, R. Jiang, K. Zhang, B. Jiang, and G. Tao, "Robust backstepping sliding-mode control and observer-based fault estimation for a quadrotor UAV," *IEEE Trans. Ind. Electron.*, vol. 63, no. 8, pp. 5044–5056, Aug. 2016.

[4] M. Rabah, A. Rohan, S. A. S. Mohamed, and S.-H. Kim, "Autonomous moving target-tracking for a UAV quadcopter based on fuzzy-PI," *IEEE Access*, vol. 7, pp. 38407–38419, Apr. 2019.

[5] H. Liu, J. Xi, and Y. Zhong, "Robust attitude stabilization for nonlinear quadrotor systems with uncertainties and delays," *IEEE Trans. Ind. Electron.*, vol. 64, no. 7, pp. 5585–5594, Jul. 2017.

[6] D. A. Ta, I. Fantoni, and R. Lozano, "Modeling and control of a tilt tri-rotor airplane," in *Proc. Amer. Control Conf. (ACC)*, Montreal, QC, Canada, Jun. 2012, pp. 131–136.

[7] S. Salazar-Cruz, F. Kendoul, R. Lozano, and I. Fantoni, "Real-time stabilization of a small three-rotor aircraft," *IEEE Trans. Aerosp. Electron. Syst.*, vol. 44, no. 2, pp. 783–794, Apr. 2008.

[8] D.-W. Yoo, H.-D. Oh, D.-Y. Won, and M.-J. Tahk, "Dynamic modeling and stabilization techniques for tri-rotor unmanned aerial vehicles," *Int. J. Aeronaut. Space Sci.*, vol. 11, no. 3, pp. 167–174, Sep. 2010.

[9] C. Papachristos, K. Alexis, and A. Tzes, "Linear quadratic optimal position control for an unmanned tri-TiltRotor," in *Proc. Int. Conf. Control, Decis. Inf. Technol. (CoDIT)*, Hammamet, Tunisia, May 2013, pp. 708–713.

[10] Z. A. Ali, D. Wang, S. Masroor, and M. S. Loya, "Attitude and altitude control of trirotor UAV by using adaptive hybrid controller," *J. Control Sci. Eng.*, vol. 2016, Jun. 2016, Art. no. 6459891.

[11] W. Ji, X. Gao, B. Xu, G. Chen, and D. Zhao, "Target recognition method of green pepper harvesting robot based on manifold ranking," *Comput. Electron. Agricult.*, vol. 177, Oct. 2020, Art. no. 105663.

[12] N. Sun, Y. Fang, H. Chen, and B. Lu, "Amplitude-saturated nonlinear output feedback antiswing control for underactuated cranes with double-pendulum cargo dynamics," *IEEE Trans. Ind. Electron.*, vol. 64, no. 3, pp. 2135–2146, Mar. 2017.

[13] N. Sun, T. Yang, Y. Fang, Y. Wu, and H. Chen, "Transportation control of double-pendulum cranes with a nonlinear quasi-PID scheme: Design and experiments," *IEEE Trans. Syst., Man, Cybern. Syst.*, vol. 49, no. 7, pp. 1408–1418, Jul. 2019.

[14] Z.-M. Li, X.-H. Chang, and J. H. Park, "Quantized static output feedback fuzzy tracking control for discrete-time nonlinear networked systems with asynchronous event-triggered constraints," *IEEE Trans. Syst., Man, Cybern. Syst.*, early access, Aug. 15, 2019, doi: 10.1109/TSMC.2019.2931530.

[15] Z.-M. Li and J. H. Park, "Dissipative fuzzy tracking control for nonlinear networked systems with quantization," *IEEE Trans. Syst., Man, Cybern. Syst.*, vol. 50, no. 12, pp. 5130–5141, Dec. 2020.

[16] H. Ramirez-Rodriguez, V. Parra-Vega, A. Sanchez-Orta, and O. Garcia-Salazar, "Robust backstepping control based on integral sliding modes for tracking of quadrotors," *J. Intell. Robot. Syst.*, vol. 73, nos. 1–4, pp. 51–66, Jan. 2014.

[17] F. Kendoul, Z. Yu, and K. Nonami, "Guidance and nonlinear control system for autonomous flight of minirotorcraft unmanned aerial vehicles," *J. Field Robot.*, vol. 27, no. 3, pp. 311–334, May 2010.

[18] T. Li, Y. Zhang, and B. W. Gordon, "Passive and active nonlinear fault-tolerant control of a quadrotor unmanned aerial vehicle based on the sliding mode control technique," *Proc. Inst. Mech. Eng., I, J. Syst. Control Eng.*, vol. 227, no. 1, pp. 12–23, Oct. 2012.

[19] F. Chen, Q. Wu, B. Jiang, and G. Tao, "A reconfiguration scheme for quadrotor helicopter via simple adaptive control and quantum logic," *IEEE Trans. Ind. Electron.*, vol. 62, no. 7, pp. 4328–4335, Jul. 2015.

[20] W. Ji, Y. Ding, B. Xu, G. Chen, and D. Zhao, "Adaptive variable parameter impedance control for apple harvesting robot compliant picking," *Complexity*, vol. 2020, Apr. 2020, Art. no. 4812657.

[21] B. Yu, Y. Zhang, I. Minchala, and Y. Qu, "Fault-tolerant control with linear quadratic and model predictive control techniques against actuator faults in a quadrotor UAV," in *Proc. Conf. Control Fault-Tolerant Syst. (SysTol)*, Nice, France, Oct. 2013, pp. 661–666.

[22] W. Hao, B. Xian, and T. Xie, "Fault tolerant position tracking control design for an tilt tri-rotor unmanned aerial vehicle," *IEEE Trans. Ind. Electron.*, early access, Jan. 14, 2021, doi: 10.1109/TIE.2021.3050384.

[23] J. Shin, H. J. Kim, Y. Kim, and W. E. Dixon, "Autonomous flight of the rotorcraft-based UAV using RISE feedback and NN feedforward terms," *IEEE Trans. Control Syst. Technol.*, vol. 20, no. 5, pp. 1392–1399, Sep. 2012.

[24] W. Hao and B. Xian, "Nonlinear fault tolerant control for a tri-rotor UAV against rear servo's stuck fault," in *Proc. 36th Chin. Control Conf. (CCC)*, Dalian, China, Jul. 2017, pp. 7109–7114.

[25] Z. Cai, M. S. deQueiroz, and D. M. Dawson, "A sufficiently smooth projection operator," *IEEE Trans. Autom. Control*, vol. 51, no. 1, pp. 135–139, Jan. 2006.

[26] E. D. Sontag, "Smooth stabilization implies coprime factorization," *IEEE Trans. Autom. Control*, vol. 34, no. 4, pp. 435–443, Apr. 1989.

[27] B. Xian, D. M. Dawson, M. S. de Queiroz, and J. Chen, "A continuous asymptotic tracking control strategy for uncertain nonlinear systems," *IEEE Trans. Autom. Control*, vol. 49, no. 7, pp. 1206–1211, Jul. 2004.

[28] B. Xian, B. Zhao, Y. Zhang, and X. Zhang, "A low-cost hardware-in-the-loop-simulation testbed of quadrotor UAV and implementation of nonlinear control schemes," *Robotica*, vol. 35, no. 3, pp. 588–612, Mar. 2017.
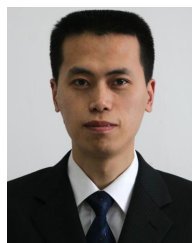
WEI YUAN received the M.S. degree from the School of Control Science and Engineering, Shandong University, Jinan, China, in 2007. He is currently pursuing the Ph.D. degree with the Nanjing University of Aeronautics and Astronautics, China. He is also with the Flying College, Binzhou University. His main research interest includes UAV's intelligent application.

WEI HAO received the B.S. degree in electrical engineering and automation from Shijiazhuang Tiedao University, Shijiazhuang, China, in 2011, the M.S. degree in navigation, guidance and control from the Civil Aviation University of China, Tianjin, China, in 2014, and the Ph.D. degree in control science and engineering from Tianjin University, Tianjin, in 2018. He is currently a Lecturer with the Flying College, Binzhou University, Binzhou, China. His main research interests include nonlinear control and fault tolerant control of unmanned aerial vehicles.

HAIJUN WANG received the M.S. degree from the School of Information Science and Engineering, Shandong University, Jinan, China, in 2007, and the Ph.D. degree in transportation engineering from the Nanjing University of Aeronautics and Astronautics, Nanjing, China, in 2020. He is currently an Associate Professor with the Flying College, Binzhou University. His main research interest includes visual tracking of multi-rotor UAVs.

WENLAI MA received the M.S. degree from the College of Information Science and Engineering, Northeastern University, Shenyang, China, in 2006. He is currently pursuing the Ph.D. degree with the Nanjing University of Aeronautics and Astronautics, China. He is also with the Flying College, Binzhou University. His main research interests include abnormal behavior and conflict of UAV.

YUJIE DU received the Ph.D. degree in electronic science and technology from the Nanjing University of Science and Technology, Nanjing, China, in 2012. He is currently a Professor with the Flying College, Binzhou University, China. His research interests include UAV's intelligent control and robust visual tracking.

• • •